

## CHARACTERIZATION AND DEGRADATION OF PEROVSKITE MINI-MODULES

R. Ebner<sup>1</sup>, A. Mittal<sup>1</sup>, G. Ujvari<sup>1</sup>, M. Hadjipanayi<sup>2</sup>, V. Paraskeva<sup>2</sup>, G. E. Georghiou<sup>2</sup>, A. Hadipour<sup>3</sup>, A. Aguirre<sup>4,5,6</sup>, T. Aernouts<sup>4,5,6</sup>, T. Fontanot<sup>7</sup>, S. Pechmann<sup>7</sup>, S. Christiansen<sup>7,8</sup>, V. Zardetto<sup>9</sup>

<sup>1</sup>AIT Austrian Institute of Technology, Center for Energy, Giefinggasse 2, 1210 Vienna, Austria, T +43 50550-6628, F +43 50550-6390, rita.ebner@ait.ac.at, www.ait.ac.at

<sup>2</sup>University of Cyprus, 1 Panepistimiou Avenue, 2109 Aglantzia, Nicosia, Cyprus, www.foss.ucy.ac.cy

<sup>3</sup>Kuwait University, Department of Physics, Condensed Matter Physics Group, University City Shadadiya Campus, Kuwait

<sup>4</sup>Imec, imo-imomec, Thin Film PV Technology – partner in Solliance, Thor Park 8320, 3600 Genk, Belgium

<sup>5</sup>EnergyVille, imo-imomec, Thor Park 8320, 3600 Genk, Belgium

<sup>6</sup>Hasselt University, imo-imomec, Martelarenlaan 42, 3500 Hasselt, Belgium

<sup>7</sup>Fraunhofer Institute for Ceramic Technologies and Systems IKTS, Äußere Nürnberger Str. 62, 91301 Forchheim, Germany, www.ikts.fraunhofer.de

<sup>8</sup>Max Planck Institute for the Science of Light, Günther-Scharowsky-Strasse 1, 91058 Erlangen, Germany, mpl.mpg.de

<sup>9</sup>TNO Energy Transition, High Tech Campus, Eindhoven, The Netherlands, valerio.zardetto@tno.nl

### ABSTRACT:

Organic-inorganic hybrid metal halide perovskites are poised to revolutionize the next generation of photovoltaics with their exceptional optoelectronic properties compatibility with low-cost and large-scale fabrication methods. The leap forward in the power conversion efficiency (PCE) enabled by lead halide perovskites is unprecedented, with PCEs emerging from 3.8% in its first study to a current certified value of 25.5% in single-junction and 33.7% in perovskite-silicon tandem devices [1-3]. The main challenge for the successful commercialization of perovskite solar cells is to achieve high stability at the module level. The commercially available solar modules undergo a series of characterization procedures that analyze their properties and ensure their quality. However, these procedures and protocols cannot unambiguously be applied to perovskite solar modules (PSM) due to its unpredictable degradation mechanisms. Therefore more advanced characterization methods are needed to understand the degradation mechanisms in the PSM. In this context, optical and electrical measurement methods are effectively employed in quality control and development support and are essential characterization tools in industry and research.

KEYWORDS: Perovskite, Optical and electrical characterization, Degradation

## 1 INTRODUCTION

In the proposed work, we employed optical and electrical characterization methods to understand the degradation of perovskite mini-modules. Optical techniques such as electroluminescence (EL), photoluminescence (PL), and dark lock-in thermography (DLIT) are non-destructive measurement techniques and provide high-resolution images showing a two-dimensional distribution of the characteristic features of PV cells and allowing the investigation of cracks, defects, shunts, and stacking faults in the cells [4]. Furthermore, electrical measurements like current-voltage (IV) characteristics and external quantum efficiency (EQE) can provide information on the power output and other device parameters, which could be used to identify the possible degradation route.

## 2 EXPERIMENTS

### 2.1 Perovskite mini-modules

A - double cation-double halide perovskite active layer with the composition  $\text{Cs}_{0.18}\text{FA}_{0.82}\text{PbI}_{2.82}\text{Br}_{0.18}$  was used. To make large-area devices, so-called mini-modules were produced by laser scribing, to generate 7 sub-cells connected in series. To prevent penetration of metallic particles of the top electrode into the soft perovskite layer, ITO (indium-tin-oxide) was used. ITO was also selected as a top electrode to obtain semi-transparent modules. The

module stack was as follows: glass/ITO/Hole transport layer (HTL)/560nm 2C Perovskite with bandgap of 1.6 eV/Electron transport layer (ETL)/ITO/glass. Fig.1 depicts the structure of the perovskite sub-cell and Fig. 2 illustrates the cross-section of the mini-module. Fig.3 shows two images of the front and back side of one perovskite mini-module (substrate size: 3cm x 3cm and module size: 2cm x 2cm) and Fig.4 shows the EL-images (front and backside) of one perovskite mini-module. Four perovskite mini-modules (“S9”, “S10”, “S11” and “S12”) were produced and characterized by applying DLIT-, EL- and PL methods alongside IV and EQE measurements.

IV measurements as well as EL measurements were performed regularly from **July 2021 (07/21) to May 2023 (05/23)** to determine the **aging behavior** of the mini-modules.

The IV measurement setup at AIT was the following:

TRI-SOL Solar Simulator 1-1.6 KW:

Class AAA (IEC 060904-9), Steady State Continuous, Air Mass Filter 1.5 Global, Typical Power Output: 100mW/cm<sup>2</sup> (1Sun) ± 20%, vary Intensity from 0 - 1.2Sun, Lamp Type and Power Xe Arc Lamp (Lamp Power:1600W), contacting with crocodile clips.

The results are presented in section 3.1.

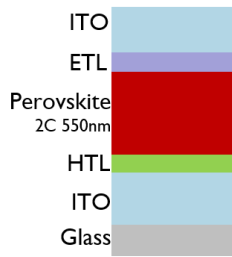


FIG.1 PIN-structure of each sub-cell.

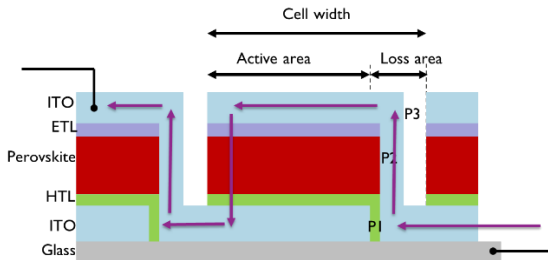


FIG.2 Cross-section of the mini-module.

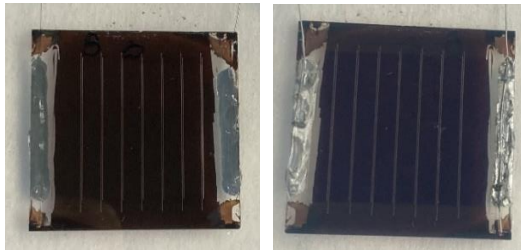


FIG.3 Perovskite mini-module: Front side (left), Back side (right).

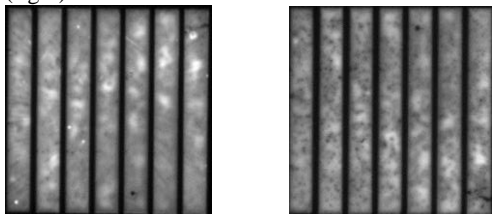


FIG.4 EL of a Perovskite mini-module: Front side (left), Back side (right).

## 2.2 Perovskite cells

The perovskite solar cell stack consists of a **glass/ITO/HTL/perovskite/passivation layer/C<sub>60</sub>/SnO<sub>x</sub>/ITO/Ag finger** in p-i-n configuration. Encapsulated semitransparent perovskite solar cells, without edge sealer and with a mask used to define the aperture area taped on the front glass, were investigated (substrate size: 2.5cm x 2.5cm and cell size: 0.5mm x 0.5mm). See the image of Sample 2 in Fig. 5 and the structure of all samples in Fig. 6.

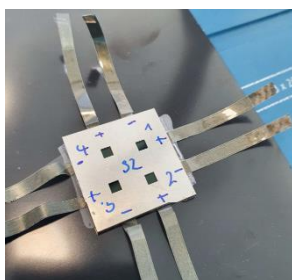


FIG.5 Four perovskite cells on Sample 2

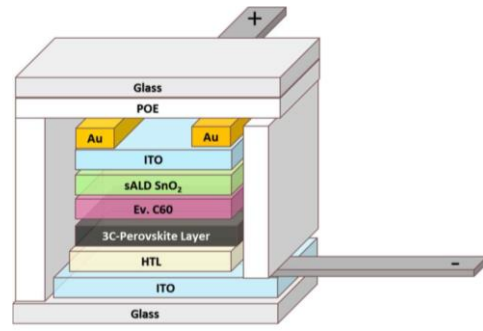


FIG.6 Structure of the perovskite sample

Four Samples with each 4 perovskite cells were produced and characterized by applying EL- and PL methods alongside IV and EQE measurements. The results are presented in section 3.2.

## 3 RESULTS

### 3.1 Perovskite mini-modules

The perovskite mini-modules were kept indoors at room temperature and measured every month. The modules were stored in the dark between the measurements. As can be seen in **Fig.7**, the mini-modules behaved in a very stable manner over this period. Only after some measurements (e.g. DLIT, Raman) there is sometimes a clear increase or decrease in power, partly reversible and also irreversible.

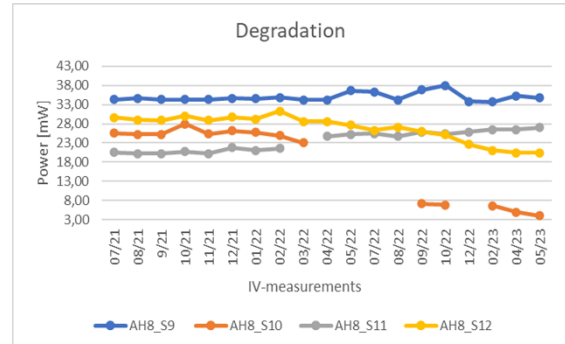


FIG.7 Aging behavior of the perovskite mini-modules

#### 3.1.1 Mini-module "S10"

Fig. 8 shows the EL images of mini-module "S10" with two inactive cells.

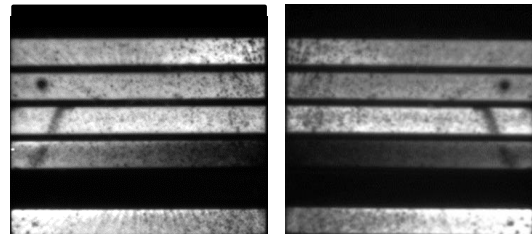


FIG.8 Perovskite mini-module "S10": Front side (left) and back side (right).

On mini-module "S10" DLIT-measurements were carried out.

##### 3.1.1.1 DLIT-measurements

DLIT measurements were carried out on the selected mini modules. However, it soon became evident that these measurements put a great strain on the modules, with the possibility to induce degradation, interrupt electrical contact or even re-establish broken contacts.

In the case of the mini-module "S10", it can be clearly seen in the EL image (see Fig.9), that an interrupted contact was reactivated, after the DLIT measurement performed on 10/2021 was carried out. After DLIT measurement there was only one inactive subcell instead of two.

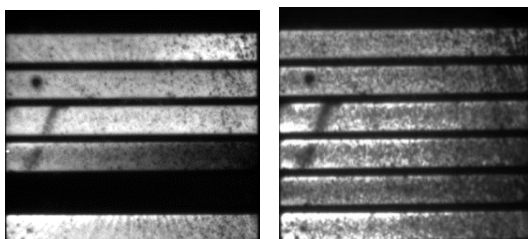


FIG.9 Mini-module "S10" before (left) and after (right) DLIT- measurement

The IV measurement results also showed a significant increase in performance after the DLIT measurement was performed (see Table 1).

Table 1: IV-measurement results of the mini-module "S10", before and after DLIT measurement (10/21).

Mini-Modul	$I_{sc}$ [mA]	$V_{oc}$ [V]	FF [%]	$P_{MPP}$ [mW]	$J_{sc}$ [mA/cm <sup>2</sup> ]
S10	10.56	6.106	39.70	25.59	13.48
S10 DLIT	10.39	6.756	39.81	27.94	13.27

However, there was already a drop in the measurement performed on 11/2021 and a subsequent return to the initial values (see Table 2).

Table 2: IV-measurements on "S10"

Mini-module	$I_{sc}$ [mA]	$V_{oc}$ [V]	FF [%]	$P_{MPP}$ [mW]	$J_{sc}$ [mA/cm <sup>2</sup> ]
S10 (initial value)	10.56	6.106	39.70	25.59	13.48
S10 DLIT Okt. 21)	10.39	6.756	39.81	27.94	13.27
S10 (Nov. 21)	10.48	6.748	38.18	26.99	13.38
S10 (Dez. 21)	10.41	6.737	37.31	26.18	13.30
S10 (Jan. 22)	10.43	6.764	36.95	25.78	13.17
S10 (Feb.22)	10.45	6.843	34.80	24.89	13.35
S10 (March 22)	10.38	6.397	34.73	23.07	13.26

After the performance of some optical measurements in April 2022 the minimodule "S10" was completely degraded (see Fig.7).

### 3.1.2 Mini-module "S11"

Fig.10 shows the EL recordings of the mini-module "S11" with three inactive cells. The IV measurement results of the mini-module "S11" are presented in Table 3.

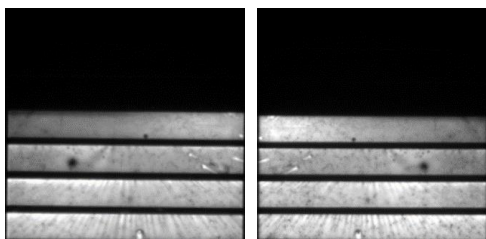


FIG.10 Perovskite mini-module "S11": Front side (left) and back side (right).

Table 3:

IV-measurement results of the mini-module "S11"

$I_{sc}$ [mA]	$V_{oc}$ [V]	FF [%]	$P_{MPP}$ [mW]	$J_{sc}$ [mA/cm <sup>2</sup> ]
10.37	5.260	37.60	20.50	13.24

In the case of the minimodule "S11", some optical measurements were carried out in March. After the return of the minimodule, a power increase (red arrow) was also determined, which is still present and further increasing (see Fig.11).

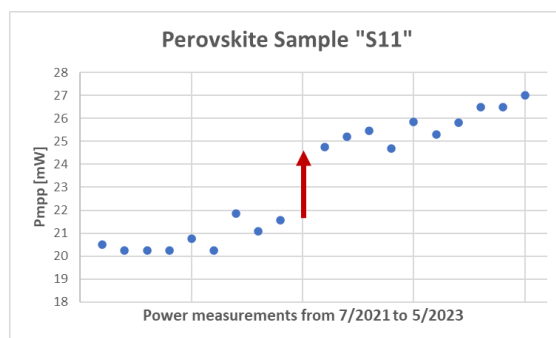


FIG.11 Performance measurements of mini-module "S11"

### 3.1.3 Mini-module "S12"

Fig.12 shows the EL images of the minimodule "S12"

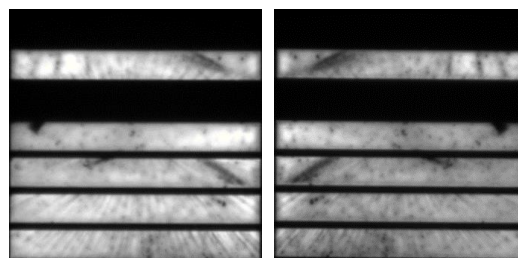


FIG.12 Perovskite mini-module "S12": Front side (left) and back side (right).

The IV measurement results of the mini-module "S12" are listed in Table 4.

Table 4:

IV-measurement results of the mini-module "S12"

$I_{sc}$ [mA]	$V_{oc}$ [V]	FF [%]	$P_{MPP}$ [mW]	$J_{sc}$ [mA/cm <sup>2</sup> ]
10.44	6.993	40.60	29.64	13.33

A significant increase in power was measured for the minimodule "S12" in February 2022. However, there was already a decrease in power in March 2022. The reason for the increase in February 2022 and the decrease in March 2022 is unclear. Since March 2022, a slight drop in performance has been noticeable for the "S12" mini-module.

### 3.2 Perovskite cells

The perovskite cells were kept indoors in a glove box between the measurements.

Fig. 13 shows the EL images of four perovskite cells (front side) of Sample 2. The appearance of the cells is very homogeneous. Only on cell 3 a defect, a dark spot, is visible.

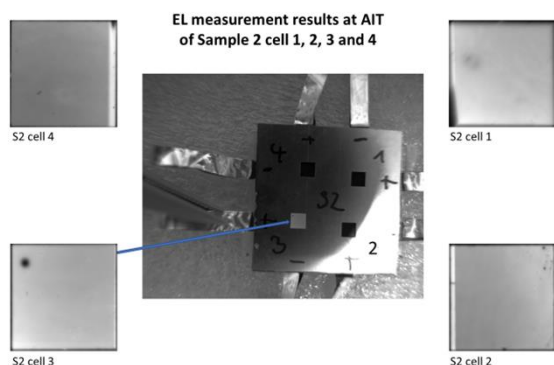


FIG.13 EL of perovskite cells, Sample 2

### 3.2.1 The IV measurement protocol

The IV measurement protocol for the perovskite cells was the following:

1. 1st JV scan from 1.2V to -0.2V and from -0.2V to 1.2V with a scan rate of 175mV/s; 20mV increment.
2. 2nd JV scan from 1.2V to -0.2V and from -0.2V to 1.2V with a scan rate of 175mV/s; 20mV increment.
3. MPPT of the (best) pixel for 180s.
4. 3rd JV scan from 1.2V to -0.2V and from -0.2V to 1.2V with a scan rate of 175mV/s; 20mV increment.

**Table 2** shows the **IV-measurement results** of cell 1 on Sample 2.

Table 2: IV-measurement results of cell 1, Sample 2

Voc [V]	Jsc [mA.cm <sup>-2</sup> ]	Pmax [mW]	FF [%]
1.117	19.94	16.8	72.65

**FIG. 14** and **FIG. 15** show the IV curves of forward and reverse measurements of cell 3 on Sample 2, according to the IV measurement protocol (see chapter 3.2.1, initial measurement 1 and final measurement 3 after MPP tracking).

Comparing the two IV curves from the initial and final measurements in Fig. 14 and 15, an improvement of the Isc and the overall cell performance after MPP tracking for 180s is achieved. The hysteresis from forward to reverse IV trace reduced from -1.9% to 0.23% from its MPP.

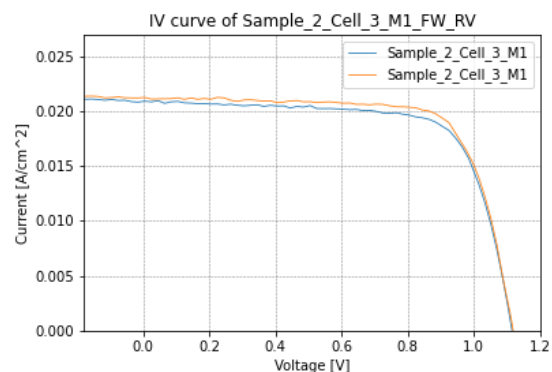


FIG.14 IV Measurement of forward and reverse curves of cell 3 on Sample 2, initial measurement

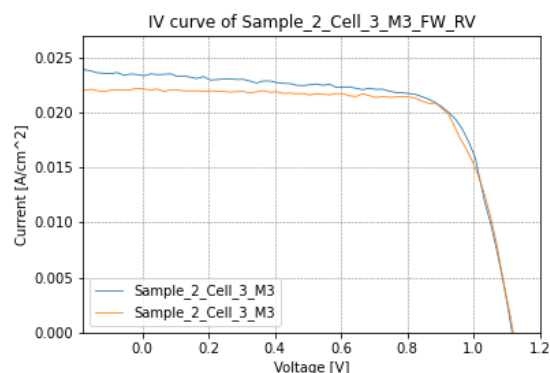


FIG.15 IV Measurement of forward and reverse curves of cell 3 on Sample 2, final measurement after the MPP tracking.

**FIG. 16** presents the **EQE** measurement results of cells from different samples.

It is clear to see that the EQE-measurement results of the cells from different samples perfectly superimpose over each other.

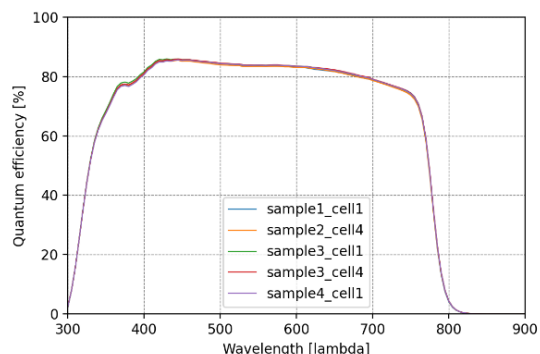


FIG.16 EQE-measurement results of 5 perovskite cells

## 4 CONCLUSIONS

Initial defects and shunts were identified by EL, PL and IV measurements.

It should be noted that some measurements (DLIT, Raman) led to an increase or decrease in power, partly reversible but also irreversible. Thus, perovskites are very sensitive to some optical measurements.

Further indoor tests and outdoor tests of differently structured perovskite samples and perovskite tandem cells have to be performed in order to identify more defects and thus be able to improve the perovskite cell and module structure. The aging behavior of the perovskite mini-modules will also be further analyzed. In addition, measurement protocols for indoor and outdoor tests of perovskites will be established.

## 5 REFERENCES

- [1] Antonio Urbina 2020 J. Phys. Energy 2 022001
- [2] "Oxford PV retakes tandem cell efficiency record", <https://www.pv->

magazine.com/2020/12/21/oxford-pv-retakes-tandem-cell-efficiency-record/

- [3] Enzheng Shi et al., “Two-dimensional halide perovskite lateral epitaxial heterostructures”, *Nature*, 2020; 580 (7805): 614
- [4] R. Ebner et al., “Non-destructive techniques for quality control of PV modules”, 39th Annual

**Acknowledgement:**

This work was funded through the European Regional Development Fund and the Republic of Cyprus in the framework of the project “**DEGRADATIONLAB**” with grant number INFRASTRUCTURES/1216/0043.  
<http://www.foss.ucy.ac.cy/degradationlab/>

“**VIPERLAB**” has received funding from the European Union’s Horizon 2020 research and innovation programme under grant agreement N°101006715